MRO INTERFEROMETER MEMO

Tip/tilt

N. Thureau, G. Loos, D. Buscher, C. Haniff

19 March 2004

OBJECTIVE:

- To determine the magnitude of the instantaneous tip-tilt motion expected at the MROI.
- To calculate the expected photon count at the MROI using the baseline tip-tilt system.
- To determine the photon count requirement for successful operation of the tip-tilt system at the MROI.
- To calculate the mechancial accuracy required for the tip-tilt actuators to deliver the necessary perfomance.
- To determine an ROM cost of a tip-tilt system for MROI.

SUMMARY:

- In order to compensate for angle of arrival variations of up to 4σ times the uncompensated atmospheric variation (for an r_0 at 0.5μm as small as 5 cm we will require an active tip-tilt mirror with a $\pm$60" tip-tilt range for its mechanical movement.
- For the nominal MROI tip-tilt sensor (an L3CCD) it will be possible to carry out interferometric measurements in the near infrared (J, H, and K) spectral bands for stars as faint as $m_V = 16$ while keeping any visibility losses due to residual tip-tilt errors to less than 10%, as long as r_0 value at 0.5μm is is larger than 5 cm.
- It will be possible to carry out interferometric measurements in the visible for stars as faint as $m_{BV} \approx 16$ if $r_0 \sim$ 15cm at 0.5μm without visibility losses (due to tip-tilt residual) greater than 10%. For poorer seeing ($r_0 \sim$ 10cm) the limiting magnitude will be about about $m_V = 15$
- Under these conditions the required accuracy for the tip-tilt motion will be 0.02 arcsec, or $\sim 0.01\mu$m in term of tip-tilt actuator motion accuracy assuming a 120 mm diameter active mirror.
- The prefered location for the tip-tilt corrector is at the telescope either as part of the telescope itself or on the optical table in the telescope enclosure.
- The prefered location for the tip-tilt sensor is on the optical table in the telescope dome. An alternative location is in the beam combiner laboratory before the delay line. This will only be possible however if the all the BVRIJHK spectral bands can be transmitted with low losses from the telescope to the beam combiner laboratory. Currently we do believe that designing suitable anti-reflection coatings to achieve this will be straightforward.

INTRODUCTION:

Astronomical measurements carried out with ground-based telescopes are corrupted by optical aberrations introduced by the Earth's atmosphere. The largest component of these aberrations are tip-tilt fluctuations. At optical interferometers these tip-tilt perturbations necessitate the use of active control of the pointing of the collimated output beams of each collector to ensure that it travels down the boresight of the beam relay pipes and is received at the beam combining laboratory. As well as this effect, uncorrected tip-tilt fluctuations lead to a reduction in visibility of the interference fringes in an interferometer, and so can have a large impact on the scientific utility of the array if the fluctuations are not controlled.

In broad terms the tip-tilt system at the MROI will consist of a sensor to measure the instantaneous wavefront errors and an active mirror to correct them. The sensor will detect the image displacement due to the atmospheric tip-tilt errors and this will be converted into measurements of the amplitude and direction of the wavefront tip-tilt. These amplitude and direction commands will then be sent to the active mirror which will be moved so as to compensate for the atmospheric tip-tilt. The tip-tilt system will be implemented as a closed feedback loop system.

1. MAGNITUDE OF THE INSTANTANEOUS TIP-TILT MOTION

We begin here by enumerating the magnitude of the tip-tilt motion expected due to the atmosphere at the MROI. The uncorrected tilt variance σ_U^2 due to the atmosphere can be written as

$$\sigma_U^2 = 0.680 \left(\frac{D}{r_0(\lambda_i)} \right)^{5/3} \left(\frac{\lambda_i}{D} \right)^2 \text{rad}^2. \tag{1}$$

Table 1 summarises the values of the expected 1-sigma tilt variation on the sky (σ_U) and the equivalent 1-sigma angle-of-arrival errors (σ_M) after taking into account the unit telescope demagnification, M. Here

$$\sigma_M = M \times \sigma_U, \tag{2}$$

and we will assume a value of M of 15 hereafter. If we design a system to correct tip-tilt variations as large as $4 \times \sigma_U$, we can see we will need an active tip-tilt mirror with a ± 60" ($\pm 280 \mu$rad) tip-tilt range.

It is useful to note that an active tip-tilt secondary mirror with comparable performance (diameter 100mm, tip-tilt range $\pm 400 \mu$rad) is a stock item available from Physik Instrumente. The same company has also delivered an 150mm active tip-tilt mirror for the Subaru telescope with a $\pm 600 \mu$rad tip-tilt range. (http://www.physikinstrumente.de/products/section3/link2.php) In view of this, we expect there to be little problem in acquiring the hardware necessary to deliver the MROI tip-tilt correction when it is needed.

r0(500nm) / cm	5	10	15
σ_U / "	0.98	0.55	0.39
σ_U / μrad	4.73	2.66	1.89
$\sigma_{M=15}$ / "	15	8	6
$\sigma_{M=15}$ / μrad	71	40	28
$\sigma_{M=20}$ / "	20	11	8
$\sigma_{M=20}$ / μrad	95	53	38

Table 1. The on-sky (σ_U) and magnified (σ_M) 1-sigma angle-of-arrival fluctuation angle expected at MROI for different seeing conditions. Values are given in both arcseconds and μradians. The nominal demagnification for the MROI is 15.

2. EXPECTED TIP-TILT VARIANCE AFTER CORRECTION

Having established what to expect from the atmosphere itself, we can now examine the expected residual variance in the angle-of-arrival fluctuations after correction, as a function of light level and seeing. We will take as our goal a need to limit the visibility loss due to uncorrected tilt errors to no more than 10%. Tango and Twiss [1980] have shown that this 10% limit corresponds to differential tilt correction errors with an angular variance of

$$\sigma^2 = 0.0784(\lambda_i/D)^2 \mathrm{rad}^2. \tag{3}$$

In practice three major sources will contribute to the residual tilt errors: anisoplanetism (σ_a), centroid uncertainty (σ_c) and temporal decorrelation (σ_t) [Sandler et al., 1994]. The total one-axis mean square tilt error can be written as the quadrature sum of these three terms:

$$\sigma_{tilt}^2 = {\sigma_a}^2 + {\sigma_c}^2 + {\sigma_t}^2 \tag{4}$$

Note that the anisoplanetism error appears if the field star used for tilt sensing is different from the science object. At the MROI we expect to perform our tip-tilt sensing on the science object itself and so hereafter we will set $\sigma_a = 0$.

2.1. Centroid error

Apart from the case of an infinitely bright source, the centroid of a target will be measured imperfectly because of the photon count fluctuations in the source signal and the sky background, and because of any detector readout noise. The rms measurement uncertainty will thus depend on the size of the source image, the photon flux from the source and the sky, and the properties of the detector.

It can be shown that for a quadrant-cell sensor the rms error in measuring the centroid of an image due to Poisson and detector readout noise is proportional to 1/SNR [Olivier and Gavel, 1994]

$$\sigma_c = \frac{3\pi}{16}\frac{1}{SNR}\frac{\lambda_t}{D}\mathrm{rad}, \tag{5}$$

where λ_t is the mean sensing wavelength, D is the diameter of the telescope and the factor SNR (the signal-to-noise-ratio for a quadrant detector) is given by:

$$SNR = \frac{N}{(4n^2+N)^{1/2}}. \tag{6}$$

Here N is the number of detected photons per basic integration and n is the rms readout noise per pixel from the sky background and the detector. For an L3CCD, $n = 0$, thus $SNR = \sqrt{N}$.

This expression for σ_c is appropriate only for a single estimate of the centroid. If centroid measurements, made at a sampling frequency $f_s = 1/\Delta t$, are used in a closed feedback loop with a 3-db bandwidth f_{3dB}, then an additional factor of γ, defined as

$$\gamma = \left[\frac{2}{\Omega} tan^{-1}\left(\frac{\Omega}{2}\right)\right]^{1/2}. \tag{7}$$

is introduced, where

$$\Omega = \frac{f_s}{f_{3dB}} = \frac{1}{\Delta t f_{3dB}}. \tag{8}$$

The factor γ accounts for the control system error [Papoulis, 1965]. This error will be large if one attempts to drive the tip-tilt feedback loop at a frequency (f_{3dB}) greater than the basic sampling rate f_s of the sensor. This reflects an important rule of typical control systems which states that the frequency of changes to the drive signal, f_{3dB}, should usually be the same as the sampling rate f_s, and certainly not any faster, i.e. $f_{3dB} \leq f_s$.

In the previous treatment we have assumed a perfect image on the quad cell. In practice, since the image we are trying to centroid is derived from a non-adaptively corrected telescope we need to replace D, the telescope diameter, with the value of r_0 at the sensing wavelength, $r_0(\lambda_t)$. Thus the error in the uncorrected centroid measurement can be written as:

$$\sigma_c = \frac{3\pi\gamma}{16}\frac{1}{SNR}\frac{\lambda_t}{r_0(\lambda_t)} = \frac{3\pi\gamma}{16}\frac{1}{\sqrt{N}}\frac{\lambda_t}{r_0(\lambda_t)}. \tag{9}$$

If we replace N in terms of the photon arrival rate N_{ph} and f_{3dB}:

$$N = N_{ph} \times \Delta t = \frac{N_{ph}}{\Omega f_{3dB}} \tag{10}$$

we can derive an alternative representation:

$$\sigma_c = \left(\frac{3\pi\gamma}{16}\right)\left(\frac{\Omega f_{3dB}}{N_{ph}}\right)^{1/2}\left(\frac{\lambda_t}{r_0(\lambda_t)}\right) \tag{11}$$

which can finally be rewritten as a function of the size of the diffraction limited image at the interferometric wavelength λ_i

$$\sigma_c = \left(\frac{3\pi\gamma D}{16 r_0(\lambda_t)}\right)\left(\frac{\lambda_t}{\lambda_i}\right)\left(\frac{\Omega f_{3dB}}{N_{ph}}\right)^{1/2}\left(\frac{\lambda_i}{D}\right). \tag{12}$$

It is interesting to look at Equation 12 to examine when the centroid error will be large. This will happen when, for example:

- N_{ph} is low: the source is too faint;
- r_0 is small: the seeing is poor and so the source image is sreead over many pixels of the detector;
- f_{3dB} is high (= large γ): the tip-tilt system is run very fast and so there is little time to collect a useful number of photons for the centroid calculation.

Conclusion: In order to minimise the centroid error for given observing conditions (seeing, telescope diameter, wavelength, source magnitude) we will need to run the tip-tilt at low frequencies.

2.2. Temporal decorrelation error

The atmosphere will change with time. The motion of the star image during integration and the time delay between measuring and correcting will thus introduce a tilt error. In a tip-tilt correcting system, image motion correction is implemented via a closed-loop servo. Tyler [1994] has shown that the error due to finite servo bandwidth is given by

$$\sigma_t = \left(\frac{f_T}{f_{3dB}}\right)\left(\frac{\lambda_i}{D}\right). \tag{13}$$

The Tyler frequency f_T (see Tyler [1994, Eq 84]) is a property of the atmospheric turbulence profile. If we assume a single layer model of average wind speed $\overline{V}$ we obtain:

$$f_T = \frac{0.081}{r_0(\lambda_i)^{5/6}D^{1/6}}\overline{V}. \tag{14}$$

The atmospheric tip-tilt fluctuation will be rapid (large f_T) with :

- a high wind speed $\overline{V}$
- a small r_0 (bad seeing)
- a small telescope aperture

The temporal decorrelation error will be large with:

- a high f_T: because the seeing is varying rapidly and it's more difficult to freeze the temporal variations of the atmosphere;
- a low f_{3dB}: the closed loop frequency is too small to account for the rapid seeing variations;

Conclusion: In order to minimise the temporal decorrelation error for given observing conditions (seeing, telescope diameter, wavelength, source magnitude) we will need to run the tip-tilt system at high frequencies.

2.3. The closed loop bandwidth f_{3dB}

Ideally, we would like to operate the tip-tilt system at a closed loop bandwidth f_{3dB} that minimises the tip-tilt residuals. If f_{3dB} is small, there is more time to collect photons then the centroid of the star will be measured more accurately. If f_{3dB} is large then it minimises the image motion during integration time as well as the time delay between a measurement and the applied correction. We need to find a compromise between a small f_{3dB} that minimises the centroid error and a large f_{3dB} that minimises the temporal decorrelation error.

A way to reach this compromise would be to use an f_{3dB} that minimises the sum of the centroid noise variance and the temporal decorrelation. This statement can be mathematically written in this way:

$$\frac{\partial(\sigma_c^2+\sigma_t^2)}{\partial f_{3dB}} = 0 \tag{15}$$

If we replace σ_c and σ_t by their expression given in eq. 12 and eq. 13 we derive:

$$f_{3dB} = 8\left[\frac{f_T r_0(\lambda_t)}{3\pi\gamma D}\left(\frac{N_{ph}}{\Omega}\right)^{1/2}\left(\frac{\lambda_i}{\lambda_t}\right)\right]^{2/3} \tag{16}$$

We show in fig. 1.a and fig. 1.b f_{3dB} as a function of the interferometric wavelength λ_i for two stellar magnitudes and different seeing conditions. We can first notice that for a given stellar magnitude f_{3dB} changes by $\pm 7\%$. f_{3dB} is larger for bright sources (small magnitude) because it takes less time to collect enough photons for the centroid calculation, which means that the tip-tilt system can be run faster and still provide a good correction. f_{3dB} is smaller for faint sources (large magnitude) because it takes more time to collect enough photons for the centroid calculation.

The slope on the left hand side of each curve is due to the aperture diameter d being limited to $7r_0(\lambda_i)$. If we were using $d = 1.4$m at all wavelengths, the curves would be straight lines at shorter wavelengths as well.

Curves in fig. 1.a and fig. 1.b have been computed assuming the use of the BV band light for tip-tilt sensing. The same curves can be computed assuming the use of the VR band for tip-tilt sensing. The curves would appear shifted toward higher values of f_{3dB}, since the VR band is larger and gives higher photons counts that the BV band.

We show in fig. 1.c and fig. 1.d f_{3dB} as a function of the stellar magnitude for a given wavelength and different seeing conditions. As the stellar magnitude increases (fainter sources), f_{3dB} decreases so that the photon counts are sufficient to compute the centroid.

For practical reasons (tip-tilt mirror mechanics, computer speed), we may limit the range of f_{3dB} from $\sim$ 10Hz up to a few tens Hz. Moreover, we don't need to run the tip-tilt system as fast as a few hundred Hz because with f_{3dB} equal to a few tens Hz, the tip-tilt residuals are already way below what we need as is illustrated in section 2.5.

Conclusion: When selecting the closed-loop frequency, the main constraint is the stellar magnitude:

- Faint sources: the centroid noise will be the main source of tip-tilt error, tip-tilt system needs to be run at low frequency so that to collect enough photons for the centroid calculation.
- Bright sources: the temporal decorrelation will be the main source of tip-tilt error, the tip-tilt system needs to be run at high frequencies in order to "freeze" the atmospheric tip-tilt variation.

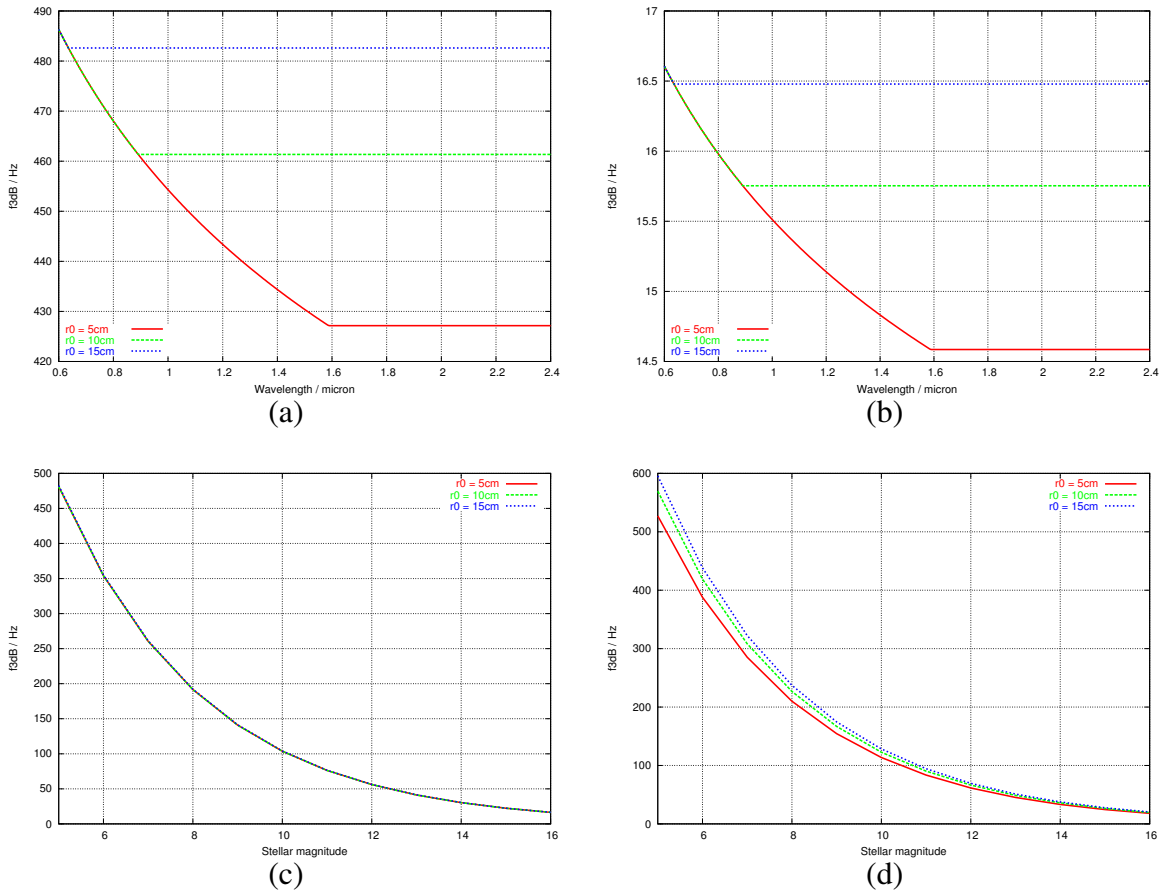

Figure 1. Plot of the closed loop bandwidth f_{3dB} computed for different seeing conditions ($r_0(0.5\mu\text{m}) = 5, 10, 14, 15\text{cm}$), $\overline{V} = 10\text{m}.s^{-1}$ and an aperture stop at $7r_0(\lambda_i)$: (a) as a function of the interferometric wavelength λ_i for a stellar magnitude of 5, with the tip-tilt sensing done in the BV band; (b) as a function of the interferometric wavelength λ_i for a stellar magnitude of 16, with the tip-tilt sensing done in the BV band; (c) as a function of the stellar magnitude at the interferometric wavelength $\lambda_i = 0.65\mu$m (only one curve is visible because the three curves overlap each other), with the tip-tilt sensing done in the BV band; (d) as a function of the stellar magnitude at the interferometric wavelength $\lambda_i = 1.65\mu$m, with the tip-tilt sensing done in the VR band.

2.4. Expected photon counts N_{ph} available to the tip-tilt sensor

In order to compute the tip-tilt residual variance for the MROI tip-tilt system, we need to calculate the number of photons per second N_{ph} that will be detected with the tip-tilt sensor as a function of the wavelength and the magnitude of the source, assuming the use of one of the two dichroics presented in Acquisition 2 memo.

Photon counts

The number of photons N_{ph} detected with the tip-tilt sensor (probably an L3CCD) is given by

$$N_{ph} = T_{opt}\,\Delta S\,\Delta t \int_{\Delta\lambda} 1.5092 \times 10^7 \frac{F_{Jy}(\lambda)T_{atm}(\lambda) \times QE(\lambda)10^{-0.4m(\lambda)}}{\lambda} d\lambda \qquad (17)$$

Wavelength /μm	Flux / Jy
0.36	1810
0.44	4260
0.55	3640
0.64	3080
0.79	2550
1.26	1600
1.60	1080
2.22	670

Wavelength /μm	Transmission
0.36	0.51
0.38	0.58
0.40	0.63
0.45	0.73
0.50	0.79
0.55	0.82
0.60	0.84
0.65	0.88
0.70	0.91
0.80	0.94
0.90	0.95
1.00	0.96

Table 2. Left table: Flux in Jansky, at m=0. Right table: Atmospheric transmission

where m is the star magnitude, T_{opt} is the transmission of the optics in the light path from the telescope to the CCD, QE is the quantum efficiency of the CCD, $\Delta S = \pi D^2/4$ the surface of the telescope, D the telescope diameter, Δt the integration time, F_{Jy} the stellar flux in Jansky (see Table 2 left hand side table), T_{atm} the atmospheric transmission (see Table 2 right hand side table), λ the wavelength, and $\Delta\lambda$ the bandwidth.
With $D = 1.4$m, $t = 1$s, QE derived from figure 9 included in section C, T_{opt} is given in table 3 and is 0.742 for a three mirror telescope and a sensor located at the telescope. We would also need to take into account the beam diffraction except for the case where the sensor is located at the telescope. With $m(\lambda) = 16$ and $\Delta\lambda$ derived from the dichroics transmission plots included in the acquisition memo, we obtain:
$N_{ph}(\text{dichroic reflects(BV)}) \sim 6900$ photons
and
$N_{ph}(\text{dichroic reflects(VR)}) \sim 11100$ photons.
These numbers would be reduced by a factor of 0.85 if the sensor would be located in the beam combiner laboratory if we had an anti-reflection coating with only 0.5% losses.

Photon counts for a typical Seyfert 1 AGN
If we consider the Seyfert 1 galaxy Mkn541 (m_B=15.5), with the flux in mJy (see table 4) from McAlary et al. [1983, Table 4, p 354], we derive the following photon counts:
$N_{ph}(\text{dichroic reflects(BV)}) \sim 7650$ photons
and
$N_{ph}(\text{dichroic reflects(VR)}) \sim 20200$ photons.
Notice that in this particular case the red colour that is typical of Seyfert means that there are many more photons in the R spectral band. The number of photons we can expect for a bright AGN of magnitude $\sim$16 is of the same order than the photon counts N_{ph} we used in order to computed the tip-tilt residual rms in the next section. As a consequence, the results presented in this section for 16th magnitude stars are applicable to AGNs.

Optics	Throughput
Telescope	0.864
ADC	0.904
Tip-tilt dichroic	0.978
Camera feed mirrors	0.986
Camera window	0.985
Total 1	0.742
Vacuum window	0.98
Relay mirrors 1&2	0.960
Delay carriage mirrors	0.941
Vacuum window	0.980
Total 2	0.644

Table 3. Transmission of the optics from the telescope to the tip-tilt sensor; The number in the row "Total 1" features the case where the tip-tilt sensor is located on the optical table in the telescope dome, "Total 2" corresponds to the case where the tip-tilt sensor is located after the delay line.

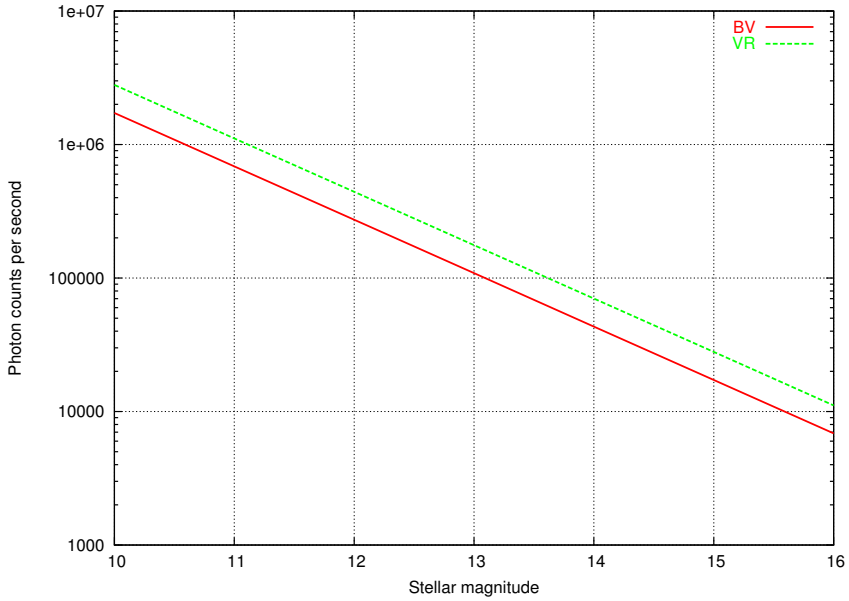

Figure 2. Plot of the photon counts per second as a function of the stellar magnitude for the two dichroics described in the acquisition memo.

2.5. Overall tip-tilt residual rms

In this section, we will discuss the overall tip-tilt residual rms, which is the quantity of interest for the description of the expected performances of a tip-tilt system. The overall tip-tilt residual variance is given by the sum of the centroid noise variance and the temporal decorrelation variance.

Aperture / "	U	B	V	R	I	Aperture / "	J	H	K
7.8	0.62	1.13	2.19	3.25	4.51	15.8	12.8	17.8	16.9

Table 4. Flux in mJansky for the Seyfert 1 galaxy Mkn541.

We show in figure 4 plots of the overall tip-tilt rms (square root of the variance) residual in arcsec as a function of the stellar magnitude in the tip-tilt sensing spectral band, at a given closed-loop frequency f_{3dB} and for different seeing conditions. In all cases we assumed: (1) the effective aperture feeding the light to the tip-tilt sensor has been truncated at $7r_0$ or 1.4m whatever is the smaller; (2) the tip-tilt sensor readout noise n is equal to 0; (3) the sampling frequency f_s is equal to f_{3dB}, i.e. $\Omega = 1$
Fig. 4.a, b, and c correspond to a situation where f_{3dB}= 50Hz whereas fig. 4.d, e, and f correspond to a situation where f_{3dB}= 15Hz.
The left hand side column corresponds to observations where the tip-tilt sensing wavelength is $\lambda_t = 0.482\mu$m (BV spectral band) and the interferometric wavelength is $\lambda_t = 0.65\mu$m (R spectral band). The thick colored line curves are the plot of the tip-tilt residual variance. The corresponding thin horizontal lines give the threshold ($= 0.28(\lambda_i/D)$) above which the visibility losses due to the tip-tilt residuals is more than 10%. The threshold is different for each value of r_0 because, the effective aperture feeding the tip-tilt sensor has been truncated at $7r_0$ (or 1.4m whatever is the smaller). The abscissa of the intercept between a thick curve and its corresponding (same colour) thin threshold line is the maximum source magnitude at which the visibility losses due to tip-tilt residuals will be lower than 10%, we will call this magnitude the limiting magnitude of our tip-tilt system.
The middle column corresponds to observations where the tip-tilt sensing wavelength is $\lambda_t = 0.7855\mu$m (VR spectral band) and the interferometric wavelength is $\lambda_t = 1.65\mu$m (H spectral band). The right hand side column corresponds to observations where the tip-tilt sensing wavelength is $\lambda_t = 0.7855\mu$m (VR spectral band) and the interferometric wavelength is $\lambda_t = 2.22\mu$m (K spectral band).

In this paragraph we will first discuss in detail figure 4.a, then comment on how a different wavelength or a different closed-loop bandwidth changes the behaviour of the overall tip-tilt residual as a function of the stellar magnitude.
The overall tip-tilt residual variance is equal to the sum of the centroid variance and the temporal decorrelation variance:

$$\sigma_{tilt}^2 = {\sigma_c}^2 + {\sigma_t}^2 \tag{18}$$

the rms is the square root of the variance, i.e. σ_{tilt}. We show in figure 3.a the plot of the temporal decorrelation rms σ_c as a function of the source magnitude in the tip-tilt sensing spectral band (here BV band), in figure 3.b the plot of the centroid rms σ_t. The thick colored line curves are the plot of the tip-tilt residual rms. The corresponding thin horizontal lines give the visibility threshold. Both variances are plotted for 4 values of r_0: 5cm, 7cm, 10cm, and 15cm. The values plotted in figure 4.a are the combination of the values plotted in figure 3.a and figure 3.b.
We can observe that for stellar magnitudes smaller than 13, the dominant source of error is the temporal decorrelation error whereas for stellar magnitudes larger than 13, the main source of error is the centroid error. The closed-loop bandwidth, f_{3dB}= 50Hz, chosen to compute the values plotted in

figure 3 is the optimum value for star of ∼13th magnitude in the tip-tilt sensing band (see fig 1.c). As a result for any fainter star, the chosen f_{3dB} is a too high frequency, the photon counts per frame are insufficient, the centroid noise dominates. For brighter sources, the photon counts are adequate, as a result the centroid noise is low. The temporal decorrelation rms does not change with the stellar magnitude since it does not depend on the photon counts for a given f_{3dB} (see eq. 13).
The predominance of one or the other source of error is reflected in the shape of the curves plotted in figure 4.a. The left hand side of the cruves corresponds to the values plotted in figure 3.a whereas the right hand side of the curves corresponds to the values plotted in figure 3.b.
With the tip-tilt sensing in the BV band and $\lambda_i = 0.65\mu$m, the limited magnitudes are: ∼13 for r_0= 5cm, ∼14 for r_0= 7cm, ∼15 for r_0= 10cm, and ∼16 for r_0= 15cm. This means that the seeing has to be good in order to achieve a good tip-tilt correction on faint sources when doing science in the visible.

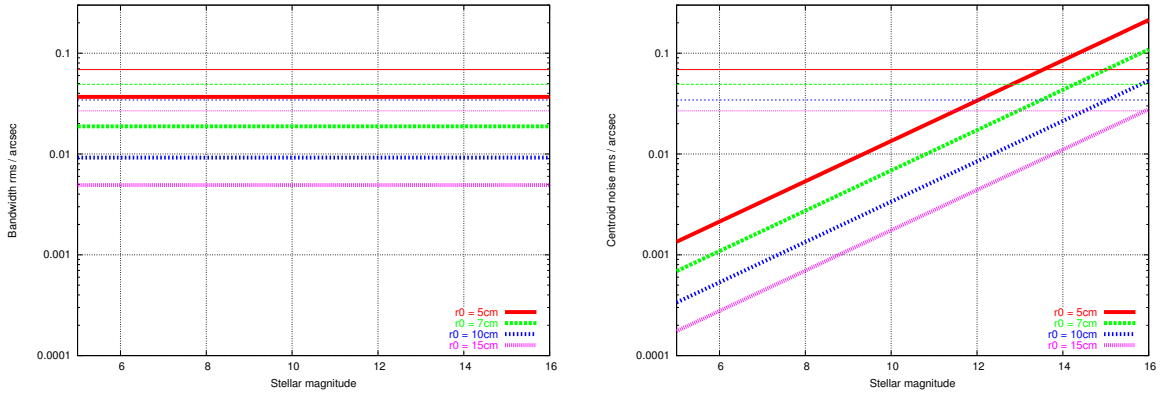

Figure 3. (a) Plot of the temporal decorrelation rms σ_c (thick lines) as a function of the source magnitude in the tip-tilt sensing spectral band (here BV band) for r_0= 0.5cm, 7cm, 10cm, and 15cm, and an interferometric wavelength $\lambda_i = 0.65\mu$m. (b) Plot of the centroid rms σ_c (thick lines) as a function of the source magnitude in the tip-tilt sensing spectral band (here BV band) for r_0= 5cm, 7cm, 10cm, and 15cm, and an interferometric wavelength $\lambda_i = 0.65\mu$m. The corresponding thin horizontal lines give the threshold ($= 0.28(\lambda_i/D)$) above which the visibility losses due to the tip-tilt error is more than 10%. In all cases: (1) the effective aperture feeding the light to the tip-tilt sensor has been truncated at $7r_0$ or 1.4m whatever is the smaller; (2) the readout noise n is assumed to be 0; (3) the sampling frequency f_s is equal to f_{3dB}, i.e. $\Omega = 1$.

Figure 4.d differs from figure 4.a because we used a smaller closed-loop bandwidth, f_{3dB} = 15Hz, for our calculations. For large stellar magnitude, the main source of error is the centroid noise. Since f_{3dB} is lower than the value used in figure 4.a, the centroid noise is expected to be smaller, i.e. a smaller frequencies corresponds to greater photon counts hence to a higher SNR in the centroid position measurement.
Because f_{3dB} is lower, the temporal decorrelation error is larger. It is so large that for r_0 = 5cm and r_0 = 7cm, the tip-tilt rms is above the threshold for the entire wavelength range. With a good seeing , r_0= 10cm, the visibility criterion is met for stellar magnitude up to 14.5. With a very good seeing, i.e. $r_0 =$ 15cm, the visibility criterion is met for the entire wavelength range.

Hence, assuming the readout noise n to be 0 and the sampling frequency f_s to be equal to f_{3dB}, it is preferable to operate the tip-tilt sytem at a higher frequency since it increases the expected limting magnitude and decreases the tip-tilt residual rms. The only exception is for observation of fainter sources in very good seing condition where the tip-tilt residual rms is minimised if using a lower frequency.

Figure 4.b differs from figure 4.a because the tip-tilt sensing is done in the VR band and the science is done in the H band ($\lambda_i = 1.65\mu$m). At this observing wavelength the atmospheric tip-tilt is changing much slowly than in the visible (f_T smaller) as a result the temporal decorrelation error is much smaller. Since the RV band is larger than the BV band and r_0 is larger in the RV band than in the BV band, the centroid noise is smaller. As before, the main source of error for brighter sources is the temporal decorrelation error whereas the main source of error for fainter soures is the centroid error. The visibility criterion is met for any stellar magnitude.
If we were using a lower closed-loop frequency, f_{3dB} = 15Hz in the same observing conditions, case illustrated in figure 4.e, the centroid noise would be smaller and the temporal decorrelation would be larger. As for the previous case, the visibility criterion is met for any stellar magnitude.
If the tip-tilt sensing is done in the VR band and the science is done in the H band, it is preferable, in order to minimise the tip-tilt residuals, to use a higher f_{3dB} when observing bright sources and marginally, use a lower f_{3dB} when observing very faint sources.

The same discussion applies to figure 4.c and figure 4.f that differ from the previous two figures because the science is done in the K band ($\lambda_i = 2.22\mu$m).

$r_0(\lambda = 0.55\mu\text{m})$ / cm	$f_{3dB} = 50Hz$			$f_{3dB} = 15Hz$		
5	13.3	16.0	>16.0	-	15.4	>16.0
7	14.2	>16.0	>16.0	-	>16.0	>16.0
10	15.0	>16.0	>16.0	14.5	>16.0	>16.0
15	16.0	>16.0	>16.0	>16.0	>16.0	>16.0

Table 5. Summary of the limited magnitude below which the visibility criterion is met. The values are taken from figure 4

Conclusion:

- The tip-tilt system will meet the visibility criterion for any observation carried out in the near infrared.
- In order to do science in the visible we will need to restrict ourselves sources brighter than 13th magnitude if the seeing is average, and observe the fainter sources only when the seeing is very good.
- A high closed-loop frequency is a better choice since it minimises the tip-tilt residual rms in most observing conditions.

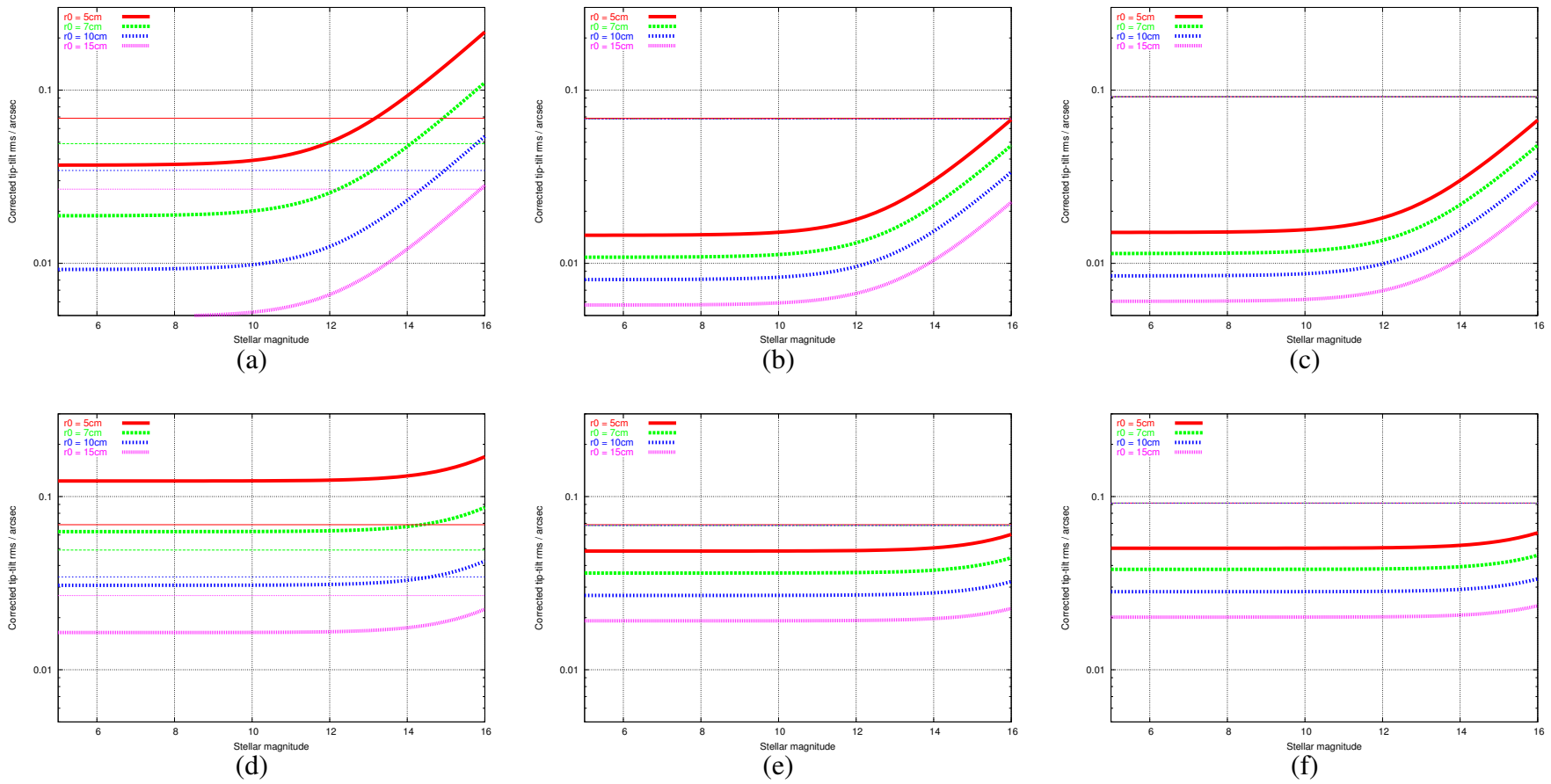

Figure 4. The thick line curves are the plots of the overall tip-tilt rms in arcsec as a function of the stellar magnitude in the tip-tilt sensing spectral band, for $r_0(0.5\mu\text{m}) = 5, 7, 10, 15\text{cm}$, average wind speed $\overline{V} = 10 m.s^{-1}$. (a) $\lambda_t = 0.48\mu$m, $\lambda_i = 0.65\mu$m, f_{3dB}=50Hz; (b) $\lambda_t = 0.78\mu$m, $\lambda_i = 1.65\mu$m, f_{3dB}=50Hz; (c) $\lambda_t = 0.78\mu$m, $\lambda_i = 2.22\mu$m, f_{3dB}=50Hz; (d) $\lambda_t = 0.48\mu$m, $\lambda_i = 0.65\mu$m, f_{3dB}=15Hz; (e) $\lambda_t = 0.78\mu$m, $\lambda_i = 1.65\mu$m, f_{3dB}=15Hz; (f)$\lambda_t = 0.78\mu$m, $\lambda_i = 2.22\mu$m, f_{3dB}=15Hz. The thin horizontal line represents the tip-tilt variance threshold $0.28(\lambda_i/D)$ in arcsec above which the visibility losses due to the tip-tilt error are more than 10%. In all cases: (1) the effective aperture feeding the light to the tip-tilt sensor has been truncated at $7r_0$ or 1.4m whatever is the smaller; (2) the readout noise n is assumed to be 0; (3) the sampling frequency f_s is equal to f_{3dB}, i.e. $\Omega = 1$

2.6. Required accuracy

One final thing that can be infered is that the tip-tilt accuracy has to be lower about one fifth of the maximum tip-tilt residual permitted by the visibility criterion (~ 0.1") so as to not limit the performance mechanically. This corresponds to ± 0.02" or $\sim \pm 0.01 \mu$m in term of tip-tilt actuator motion accuracy.

3. LOCATION OF THE TIP-TILT SENSOR AND CORRECTOR

A tip-tilt system comprises two subsystems:

1. A corrector: Usually a mirror that is tip-tilted by mean of a set of actuators located at the back of the mirror.
2. A sensor: A detector which records the image of the source, the image is processed and the tip-tilt correction to be applied is computed.

In this section, we discuss the possible location of this two sub-systems, knowing that the tip-tilt mirror **must** be located **before** the tip-tilt sensor in the optical train.
The chosen location for each of the sub-sytem will impact on the size of pipes and optics all the way from the telescope to the beam combiner. They will have to be large enough to accomodate:

- $\pm 4 \times \sigma_U$ from the telescope to the tip-tilt mirror, in order to be able to correct the tip-tilt 99.9% of the time;
- $\pm 2 \times \sigma_U$ from the telescope to the tip-tilt sensor, so that the star can be acquired, and the tip-tilt system can lock on the star and switch into the closed loop mode;
- $\pm 3 \times \sigma_{tilt}$ from the telecope to the beam combiner, so that the star can be detected 99% of the time.

with $\pm 4 \times \sigma_U > \pm 2 \times \sigma_U > \pm 3 \times \sigma_{tilt}$.

3.1. Location of the tip-tilt corrector

The tip-tilt correctors could in principle be located either at the telescope, on the optical table in the telescope dome or in the beam combining laboratory either before or after the delay lines.

3.1.1. In the beam combiner laboratory, after the delay lines

If the correction were to take place in the beam combiner (BC) laboratory after the delay line, the optics and the pipes from the telescope to the tip-tilt corrector would have to accomodate a $\pm 4 \times \sigma_U = \pm 60''$ atmospheric tip-tilt angle. A 4σ atmospheric tip-tilt angle of 60" would lead to a $\sim \pm$165mm beam displacement after the delay lines. This number has been computed assuming that the telescope is on a foundation 200m away from the array centre and that the optical path length in the delay line system is 360m.
Such a beam displacement is even larger than the beam diameter itself. Even if we had optics/pipes large enough to accommodate the $\pm 4 \times \sigma_U$ angle, and decided to apply the tip-tilt correction after the dealy line, the beam displacement would most of the time be so large that the light beams would not enter the miniature beam combiner and/or not overlap.

3.1.2. In the beam combiner laboratory, before the delay lines

If the correction were to take place in the BC laboratory before the delay line, the optics and the pipes from the telescope to the tip-tilt corrector would have to accomodate a $\pm 4 \times \sigma_U = \pm 60''$ atmospheric tip-tilt angle. A 4σ atmospheric tip-tilt angle of 60" would lead to a $\sim \pm$62mm beam displacement after the delay lines. This number has been computed assuming that the telescope is on a foundation 200m away from the array centre.
Such a beam displacement is about 67% of the beam diameter itself. Even if we had optics/pipes large enough to accommodate the $\pm 4 \times \sigma_U$ angle, and decided to apply the tip-tilt correction before the dealy line, the beam displacement would most of the time be so large that the light beams would be very obstructed when entering the miniature beam combiner and would not not overlap very well causing dramatic losses in visibility of about 50%.

3.1.3. On the optical table, in the telescope dome

If the correction were to take place, on the optical table located in the telescope dome, a 4σ atmospheric tip-tilt angle of 60" would lead to a $\sim \pm$3mm beam displacement. This number has been computed assuming that the tip-tilt mirror would be located about 4m after the telescope tertiary. Such a beam displacement would not significantly impact on the size of the optics in the optical train before the tip-tilt mirror. A 3mm beam displacement is about 3% of the beam diameter, which results in visibility losses not larger than 2%.

3.1.4. In the telescope

Either the secondary or the tertiary mirror (if we assume a 3 mirror telescope design) could be used as tip-tilt corrector.
The utilisation of an active secondary as tip-tilt corrector is quite standard in astronomical telescopes (the ESO 2.2m at La Silla, the Keck outriggers, the CHARA unit telescopes) and doesn't present any particular difficulties. The mounts/mechanics of such active mirrors are compact and wouldn't increase the telescope obstruction. However, we are concerned that depending on the telescope assembly (parabola-parabola or dall-kirkham) the choice of an active secondary may not be compatible with the telescope alignement requirement.
The utilisation of an active tertiary would be complicated by the fact that this mirror is articulated and significantly larger than the secondary.

r0 (λ = 0.55 μm) / cm	before DL	after DL
5	62.38	164.55
10	35.14	92.70
15	24.6	64.89

Table 6. Summary of the oversize factor required if the tip-tilt sensor is located in the beam combiner laboratory before the delay line (middle column) or after the delay line (right hand side column). These numbers have been computed assuming that the telescope is on a foundation 200m away from the array centre, and that the optical path length in the delay line system is 360m.

Conclusion: We have to rule out the first two location we discussed because of (1) the huge beam displacement that would occur (2) the cost of very large pipes and optics (see section section).
The prefered location would be the telescope secondary, an active mirror located on the telescope optical table being a possible altenative location.

3.2. Location of the tip-tilt sensor

The tip-tilt sensor could be located either at the telescope or in the BC laboratory, as long as it is located after the tip-tilt corrector. The chosen location must satisfy several requirements that are described in the following subsections.

3.2.1. The Field of View (FOV)

In open loop, the field of view available for the tip-tilt sensor must be sufficient so that a) the star can be acquired, b) the tip-tilt system can lock on the star and switch into the closed loop mode. As a consequence, the optics and pipes in the optical train from the telescope to the tip-tilt sensor will have to be large enough to ensure that the sensor collects uncorrected light form the source. Optics and pipes that accommodate a $\pm 2 \times \sigma_U = \pm 30''$ would be required.
On the optical table in the telescope dome:
The fov of the tip-tilt sensor is roughly the same as the fov of the telescope. This argue for a parabolla-parabolla optical configuration where the fov would typically be 60arcsecs.
In the BC laboratory before the delay lines:
The tip-tilt fov would be limited by the size of the pipes and the optics. A solution to this problem would be the purchase of larger optics and pipes. If we assume the telescope to be on a foundation 200m away from the array centre, a $\pm 2 \times \sigma_U$ atmospheric tip-tilt of $\pm 30''$ would correspond to a $\sim$ 31mm beam displacement. The pipes and optics would have to be enlarged by $\sim$ 62mm (see table 6).
In the BC laboratory after the delay lines:
If we assume the telescope to be on a foundation 200m away from the array centre, and that the optical path length in the delay line system is 360m, a $\pm 2 \times \sigma_U$ atmospheric tip-tilt of $\pm 30''$ would correspond to a $\sim$ 82mm beam displacement. The pipes and optics would have to be enlarged by $\sim$ 165mm (see table 6).

Conclusion: The ovesized factor associated to the tip-tilt sensor being located in the beam combiner laboratory is very large.

3.2.2. Photons requirement

The number of photons delivered by the tip-tilt sensor will be affected by teh tip-tilt location in the following way.

At the telescope:

This location minimises the number of optics between the telescope and the sensor, which maximises the number of photons available for tip-tilt sensing.

In the BC lab:

The flux collected by the tip-tilt sensors would be reduced compared to the flux available for a tip-tilt sensor located at the telescope. This attenuation would be due both to the greater number of optics in the optical path (7 more optics:) and to the diffraction which would cause about 5% flux loss for a 200m optical path length and 10% for a 600m optical path length [Horton et al., 2001]. There is also an uncertainty on the achievable transmission for anti-reflexion coating. In the original plans, we assumed we would use BV band light for tip-tilt sensing while doing science in the visible, and VR band light for tip-tilt sensing while doing science in the near infrared. It might be quite difficult to make anti-reflection coatings that transmit all the light from the B band to the K band to the BC lab unless we are ready to compromise on the quality of the coating. The current anti-reflection coatings have 0.5% losses, a new coating would have significantly higher losses.

Conclusion: There are clear benefits to put the tip-tilt sensor at the telescope.

3.2.3. The quality of the tip-tilt correction

The location of the tip-tilt sensor will impact on the quality of the tip-tilt sesning in the following way.

At the telescope:

The tip-tilt sensors would detect the atmospheric perturbation occurring in the beam path from the star to the telescope.

In the BC lab:

The tip-tilt sensor would additionally detect the tip-tilt perturbation occurring in the beam path from the telescope to the beam combiner.

Conclusion: If we were only worrying about the quality of the tip-tilt correction, we would put the tip-tilt sensor in the beam combiner laboratory.

3.2.4. The cost

The main objective is to deliver a fully operational tip-tilt system that satisfy the scientific requirements within the available budget. If the tip-tilt sensors were to be located in the BC lab, we would need to purchase

- larger optics, pipes and trolleys;
- more complex anti-reflexion coatings;
- 11 acquisition cameras at the telescope to be sure that the beam goes in the BC laboratory. (amateur CCDs, same as for the pointing system).

See section 4 for a detailed costing of the different options.

If the sensors are in the beam combiner laboratory, then one potential cost saving would arise from sending several beams on the same L3CCD. The approxmate saving on 5 L3CCDs is about -160-190k$

4. COST OF A TIP-TILT SYSTEM FOR MROI

In this final part of the memo, we examine the approximate cost of a tip-tilt system considering 3 cases:

- Tip-tilt sensor and tip-tilt mirror at the telescope
- Tip-tilt mirror at the telescope and tip-tilt sensor in the beam combiner laboratory before the delay lines.
- Tip-tilt mirror at the telescope and tip-tilt sensor in the beam combiner laboratory after the delay lines.

The pipes and optics in the light beam from the telescope to the beam combiner must be large enough to accommodate the beam displacements due to the uncorrected tip-tilt and tip-tilt residuals. In order to get optics/pipes large enough we will need to oversize their sizes compared to the beam diameter. If d is the size of the beam, $d+\delta$ is the final size of the optics/pipes, where δ is $2\times$the maximum beam displacement. From the telescope to the tip-tilt sensor, $d+\delta$ must accomodate $\pm 2\sigma_U$, in order to catch the beam often enough to close the tip-tilt control loop, where σ_U is the uncorrected tip-tilt rms. From the telescope to the beam combiner, $d+\delta$ must be large enough to accomodate $\pm 3\sigma_{tilt}$, in order to optimise the light output, where σ_{tilt} is the residual tip-tilt rms, after correction. For the moment I investigated the required size for:

- 1 relay mirror located near the telescope
- 1 window near the telescope
- 1 relay mirror close to the building
- pipes from the telescope to the building
- delay line pipes
- delay line cat's eye pimary
- 1 window for the beam to exit the delay line
- 1 relay after the delay line

, assuming a telescope magnification $M = 15$. There are also two addionnal windows required in the case where the tip-tilt sensor is located in the BC laboratory before the delay lines.

	At the telescope	In the BC laboratory	
		Before the DL	After the DL
Relay 1	5"	5"	5"
Window 1	5"	5"	5"
Relay 2	5"	7"	7"
Outdoor pipes	OD 6" / W .25"	OD 9" / W .25"	OD 9" / W .25"
Indoor pipes	OD 18" / W .50"	OD 18" / W .50"	OD 33" / W .50"
Delay line primary	12"	12"	21"
Window 2	5"	5"	11"
Relay 3	5"	5"	11"
Outdoor pipes exit window	-	7"	-
Indoor pipes input window	-	5"	-

Table 7. Estimated size for the optics and pipes for the three possible tip-tilt sensor locations: at the telescope, in the beam combiner lab before or after the delay lines.

	At the telescope	In the BC laboratory	
		Before the DL	After the DL
Relay 1 $\times 11$	4.4	4.4	4.4
Window 1 $\times 11$	9.24	9.24	29.7
Relay 2 $\times 11$	4.4	9.35	9.35
Outdoor pipes 1600m	45.3	75.9	75.9
Indoor pipes 1800m	320.3	320.3	587.2
Delay line primary $\times 11$	6	6	18*
Window 2 $\times 11$	9.24	9.24	45*
Relay 3 $\times 11$	4.4	4.4	43.55*
Outdoor pipes exit window	-	18*	-
Indoor pipes input window	-	9.24	-
Total	403	466	813

Table 8. Preliminary costing in k$. * : priced guessed from quote for smaller optics, scaled a a function of the surface.

Conclusion: There is not a major cost difference between a tip-tilt system with a sensor located on the optical table in the telescope dome and a tip-tilt system with a sensor located in the beam combiner laboratory before the delay line. However, these prices do not include the cost of the new anti-reflection coating we would need if the sensor were to be located in the beam combiner laboratory.
A tip-tilt system with a sensor located in the beam combiner laboratory after the delay line would be twice more expensive.

APPENDIX A. TIP-TILT RESIDUAL RMS DEPENDENCE ON READOUT NOISE AND SAMPLING FREQUENCY

In this section we present a set a curves similar to those presented in figure 4 section 2.5, which we calculated in order to investigate the dependency of the tip-tilt rms residual upon the tip-tilt sensor read-out noise and the sampling frequency.

A.1. $n = 2, \Omega = 1$

In this section, we set the tip-tilt sensor read-out noise per pixel to be equal to 2 while the sampling frequency f_s is kept equal to f_{3dB} ($\Omega = 1$). As a result, the SNR will be reduced compared to the case where we had $n = 0$ (see figure 4), which will increase the centroid error while the temporal decorrelation error is unchanged. Hence, the tip-tilt residual will be unchanged for bright sources and will increase for faint sources as illustrated in figure 5.

$r_0(\lambda = 0.55\mu\text{m})$ / cm	$f_{3dB} = 50Hz$			$f_{3dB} = 15Hz$		
5	13.2	16.0	>16.0	-	>16.0	>16.0
7	14.0	>16.0	>16.0	-	>16.0	>16.0
10	15.0	>16.0	>16.0	14.6	>16.0	>16.0
15	15.8	>16.0	>16.0	14.6	>16.0	>16.0

Table 9. Summary of the limited magnitude below which the visibility criterion is met. The values are taken from figure 5 and can be compared to values presented in table 5.

A.2. $n = 0, \Omega = 10$

In this section, we set the tip-tilt sensor read-out noise per pixel to be equal to 0 while the sampling frequency f_s is equal to $10 \times f_{3dB}$ ($\Omega = 10$). As a result, the SNR will be reduced, the SNR will be reduced compared to the case where we had $\Omega = 1$ (see figure 4) which will increase the centroid error while the temporal decorrelation error is unchanged. Hence, the tip-tilt residual will be unchanged for bright sources and will increase for faint sources as illustrated in figure 6. While $n = 2$ did not change very much the centroid noise for interferometric wavelengths in the near-infrared, $\Omega = 10$ degrades the tip-tilt residuals rms significantly and reduces the limiting magnitude.

$r_0(\lambda = 0.55\mu\text{m})$ / cm	$f_{3dB} = 50Hz$			$f_{3dB} = 15Hz$		
5	12.0	14.9	15.6	-	15.5	>16.0
7	13.0	15.7	>16.0	-	>16.0	>16.0
10	13.9	>16.0	>16.0	13.5	>16.0	>16.0
15	14.8	>16.0	>16.0	15.6	>16.0	>16.0

Table 10. Summary of the limited magnitude below which the visibility criterion is met. The values are taken from figure 6 and can be compared to values presented in table 5.

A.3. $n = 2$, $\Omega = 10$

In this section, we set the tip-tilt sensor read-out noise per pixel to be equal to 2 while the sampling frequency f_s is equal to $10 \times f_{3dB}$ ($\Omega = 10$). As a result, the SNR will be reduced compared to the case where we had $n = 0$ and $\Omega = 1$ (see figure 4), which will increase the centroid error while the temporal decorrelation error is unchanged. Hence, the tip-tilt residual will be unchanged for bright sources and will increase for faint sources as illustrated in figure 7. With an increased read-out noise, the tip-tilt residuals rms is much more sensitive to any change in Ω.

$r_0(\lambda = 0.55\mu\text{m})$ / cm	$f_{3dB} = 50Hz$			$f_{3dB} = 15Hz$		
5	11.9	14.6	15.3	-	15.4	>16.0
7	12.8	15.3	15.8	-	>16.0	>16.0
10	13.7	15.8	>16.0	13.4	>16.0	>16.0
15	14.5	>16.0	>16.0	15.4	>16.0	>16.0

Table 11. Summary of the limited magnitude below which the visibility criterion is met. The values are taken from figure 7 and can be compared to values presented in table 5.

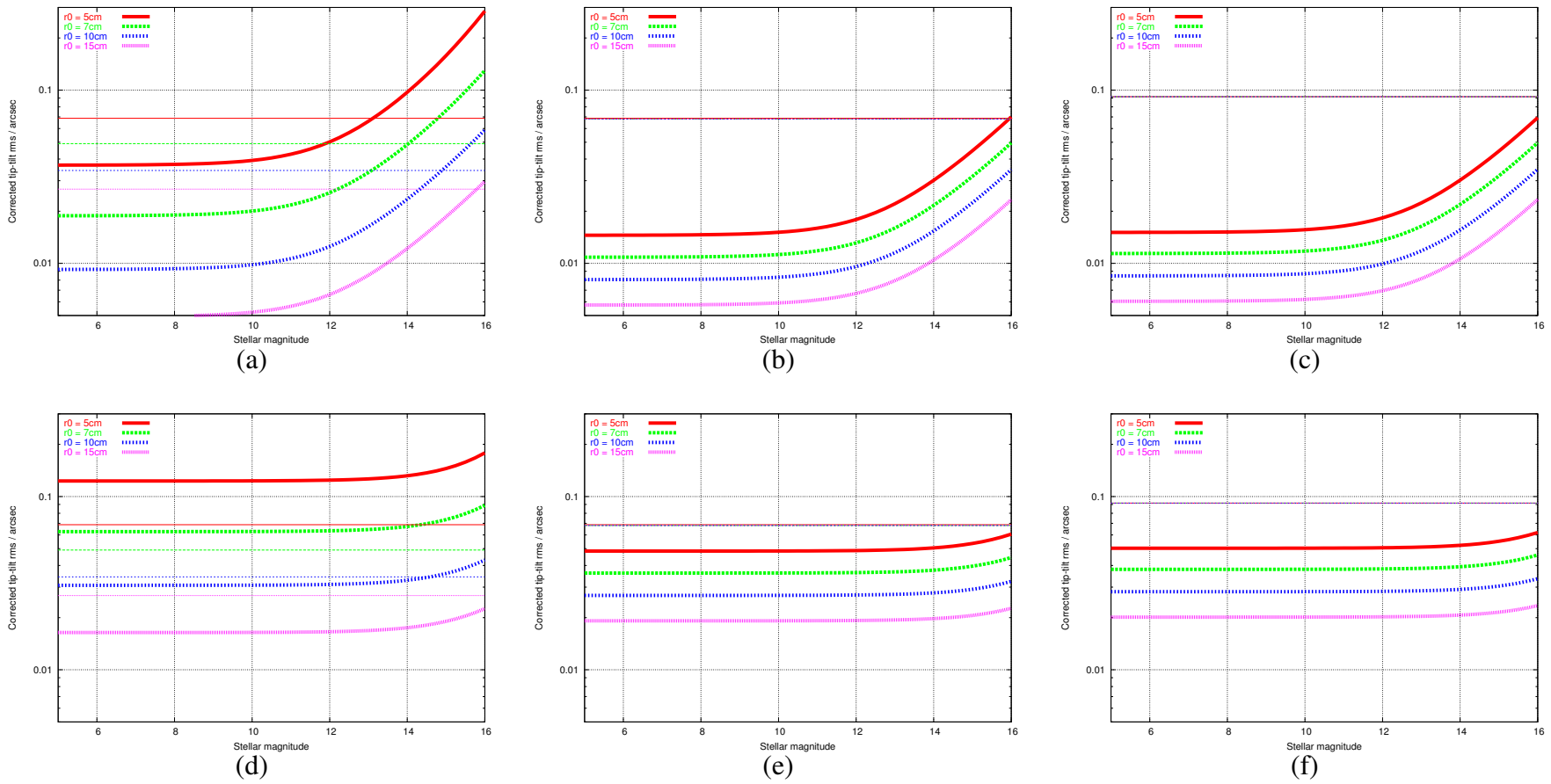

Figure 5. The thick line curves are the plots of the overall tip-tilt rms in arcsec as a function of the stellar magnitude in the tip-tilt sensing spectral band, for $r_0(0.5\mu\text{m}) = 5, 7, 10, 15\text{cm}$, average wind speed $\overline{V} = 10 m.s^{-1}$. (a) $\lambda_t = 0.48\mu$m, $\lambda_i = 0.65\mu$m, f_{3dB}=50Hz; (b) $\lambda_t = 0.78\mu$m, $\lambda_i = 1.65\mu$m, f_{3dB}=50Hz; (c) $\lambda_t = 0.78\mu$m, $\lambda_i = 2.22\mu$m, f_{3dB}=50Hz; (d) $\lambda_t = 0.48\mu$m, $\lambda_i = 0.65\mu$m, f_{3dB}=15Hz; (e) $\lambda_t = 0.78\mu$m, $\lambda_i = 1.65\mu$m, f_{3dB}=15Hz; (f)$\lambda_t = 0.78\mu$m, $\lambda_i = 2.22\mu$m, f_{3dB}=15Hz. The thin horizontal line represents the tip-tilt variance threshold $0.28(\lambda_i/D)$ in arcsec above which the visibility losses due to the tip-tilt error are more than 10%. In all cases: (1) the effective aperture feeding the light to the tip-tilt sensor has been truncated at $7r_0$ or 1.4m whatever is the smaller; (2) the readout noise n is assumed to be 2; (3) the sampling frequency f_s is equal to f_{3dB}, i.e. $\Omega = 1$

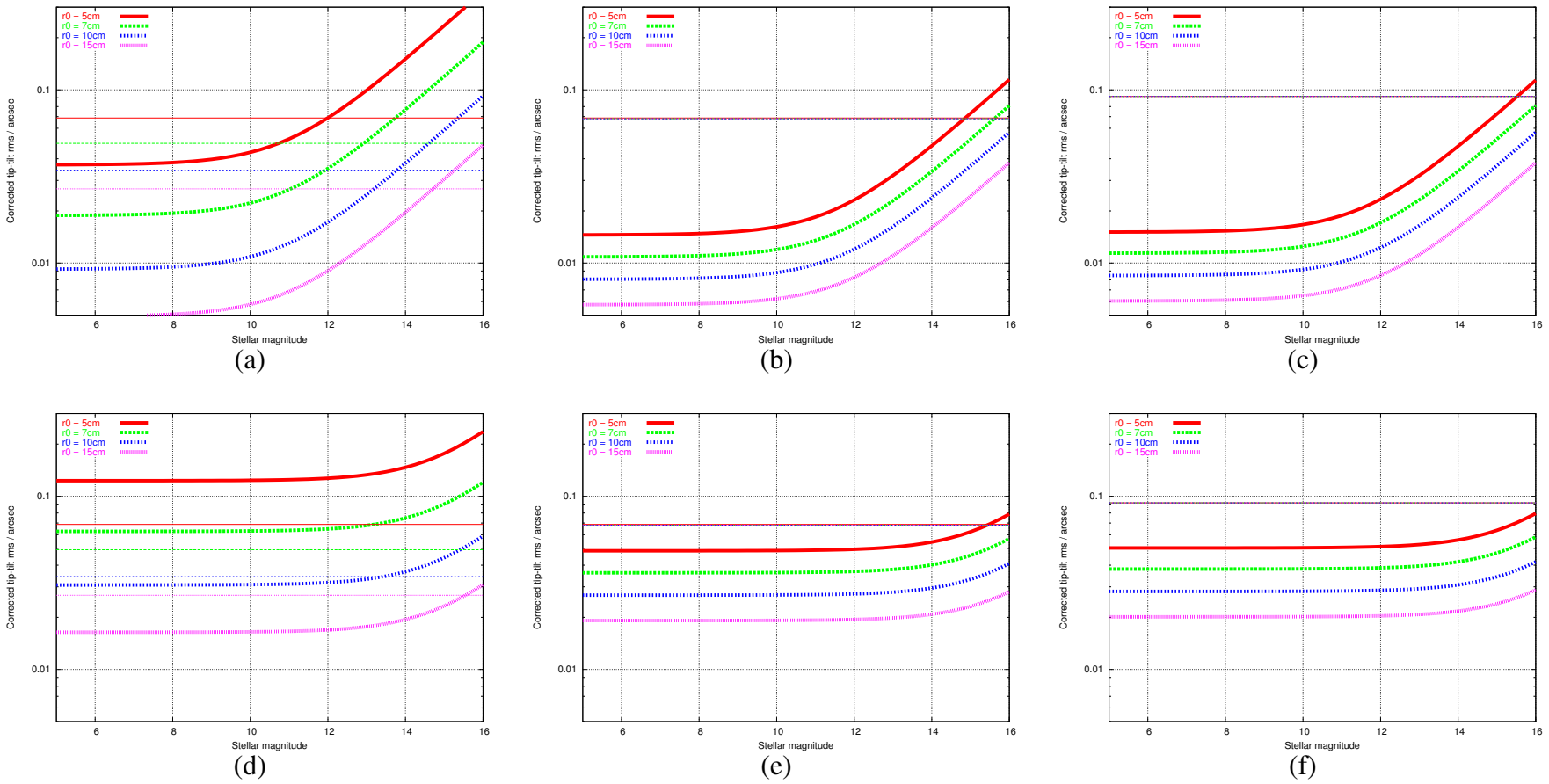

Figure 6. The thick line curves are the plots of the overall tip-tilt rms in arcsec as a function of the stellar magnitude in the tip-tilt sensing spectral band, for $r_0(0.5\mu\text{m}) = 5, 7, 10, 15$cm, average wind speed $\overline{V} = 10m.s^{-1}$. (a) $\lambda_t = 0.48\mu$m, $\lambda_i = 0.65\mu$m, f_{3dB}=50Hz; (b) $\lambda_t = 0.78\mu$m, $\lambda_i = 1.65\mu$m, f_{3dB}=50Hz; (c) $\lambda_t = 0.78\mu$m, $\lambda_i = 2.22\mu$m, f_{3dB}=50Hz; (d) $\lambda_t = 0.48\mu$m, $\lambda_i = 0.65\mu$m, f_{3dB}=15Hz; (e) $\lambda_t = 0.78\mu$m, $\lambda_i = 1.65\mu$m, f_{3dB}=15Hz; (f)$\lambda_t = 0.78\mu$m, $\lambda_i = 2.22\mu$m, f_{3dB}=15Hz. The thin horizontal line represents the tip-tilt variance threshold $0.28(\lambda_i/D)$ in arcsec above which the visibility losses due to the tip-tilt error are more than 10%. In all cases: (1) the effective aperture feeding the light to the tip-tilt sensor has been truncated at $7r_0$ or 1.4m whatever is the smaller; (2) the readout noise n is assumed to be 0; (3) the sampling frequency f_s is equal to $10 \times f_{3dB}$, i.e. $\Omega = 10$

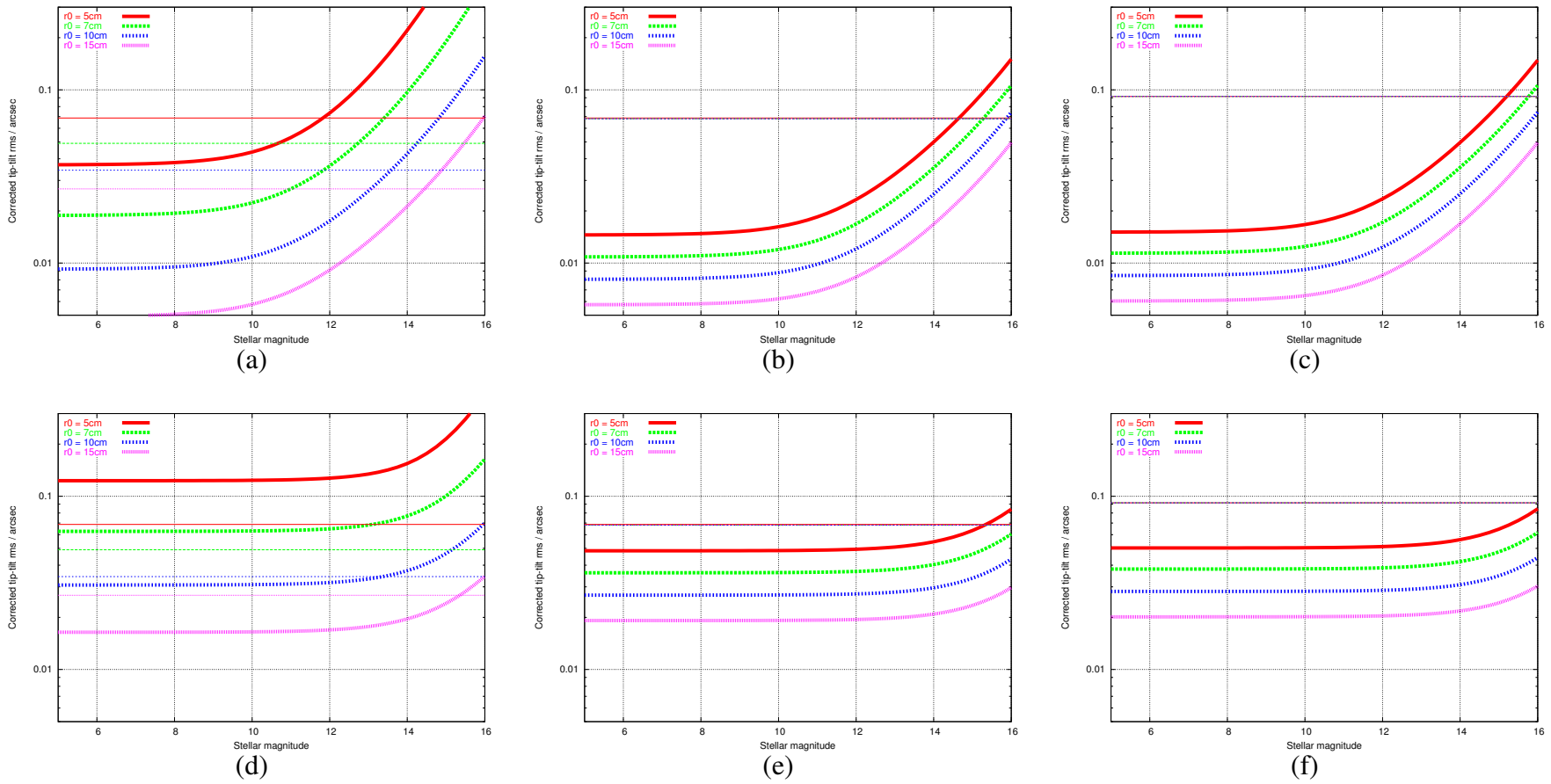

Figure 7. The thick line curves are the plots of the overall tip-tilt rms in arcsec as a function of the stellar magnitude in the tip-tilt sensing spectral band, for $r_0(0.5\mu\text{m}) = 5, 7, 10, 15\text{cm}$, average wind speed $\overline{V} = 10 m.s^{-1}$. (a) $\lambda_t = 0.48\mu$m, $\lambda_i = 0.65\mu$m, f_{3dB}=50Hz; (b) $\lambda_t = 0.78\mu$m, $\lambda_i = 1.65\mu$m, f_{3dB}=50Hz; (c) $\lambda_t = 0.78\mu$m, $\lambda_i = 2.22\mu$m, f_{3dB}=50Hz; (d) $\lambda_t = 0.48\mu$m, $\lambda_i = 0.65\mu$m, f_{3dB}=15Hz; (e) $\lambda_t = 0.78\mu$m, $\lambda_i = 1.65\mu$m, f_{3dB}=15Hz; (f)$\lambda_t = 0.78\mu$m, $\lambda_i = 2.22\mu$m, f_{3dB}=15Hz. The thin horizontal line represents the tip-tilt variance threshold $0.28(\lambda_i/D)$ in arcsec above which the visibility losses due to the tip-tilt error are more than 10%. In all cases: (1) the effective aperture feeding the light to the tip-tilt sensor has been truncated at $7r_0$ or 1.4m whatever is the smaller; (2) the readout noise n is assumed to be 2; (3) the sampling frequency f_s is equal to $10 \times_f 3dB$, i.e. $\Omega = 10$

APPENDIX B. TIP-TILT STREHL RATIO

The Strehl ratio can as well be used to check the performance of a tip-tilt system. The strehl ratio S is estimated from the expected tip-tilt variance $\sigma^2 = \sigma_c^2 + \sigma_t^2$:

$$S = exp(-(\sigma_c^2 + \sigma_t^2)) \tag{19}$$

We show in figure 8 the expected strehl ratio for the MROI tip-tilt system as a function of the stellar V magnitude for $r_0(0.5\mu\text{m}) = 5, 7, 10, 15\text{cm}$.

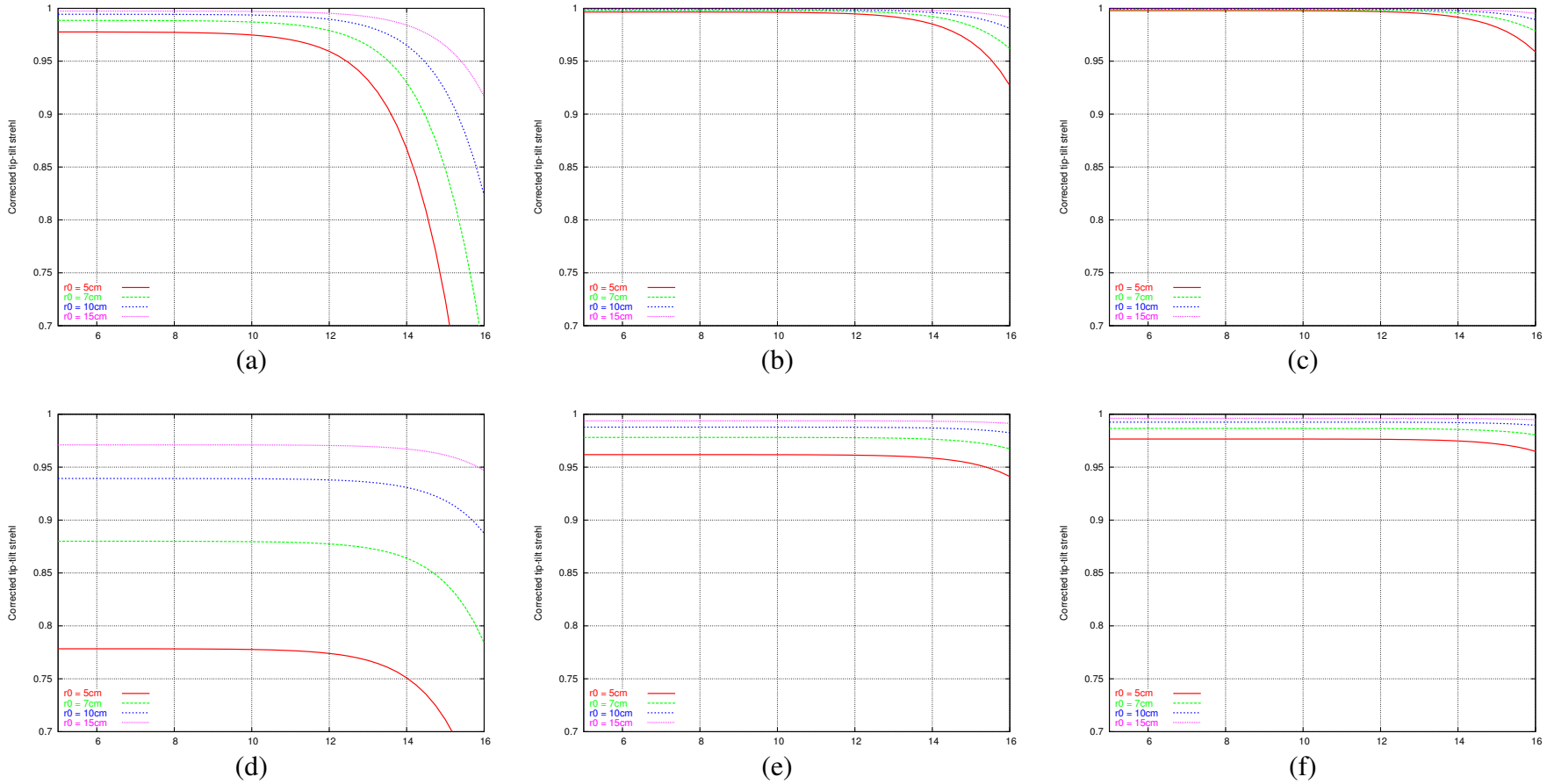

Figure 8. Plot of the tip-tilt strehl ratio S as a function of the stellar magnitude in the tip-tilt sensing spectral band, for $r_0(0.5\mu\text{m}) = 5, 7, 10, 15\text{cm}$, average wind speed $\overline{V} = 10m.s^{-1}$. (a) $\lambda_t = 0.48\mu$m, $\lambda_i = 0.65\mu$m, f_{3dB}=50Hz; (b) $\lambda_t = 0.78\mu$m, $\lambda_i = 1.65\mu$m, f_{3dB}=50Hz; (c) $\lambda_t = 0.78\mu$m, $\lambda_i = 2.22\mu$m, f_{3dB}=50Hz; (d) $\lambda_t = 0.48\mu$m, $\lambda_i = 0.65\mu$m, f_{3dB}=15Hz; (e) $\lambda_t = 0.78\mu$m, $\lambda_i = 1.65\mu$m, f_{3dB}=15Hz; (f)$\lambda_t = 0.78\mu$m, $\lambda_i = 2.22\mu$m, f_{3dB}=15Hz. In all cases: (1) the effective aperture feeding the light to the tip-tilt sensor has been truncated at $7r_0$ or 1.4m whatever is the smaller; (2) the readout noise n is assumed to be 0; (3) the sampling frequency f_s is equal to $f3dB$, i.e. $\Omega = 1$.

APPENDIX C. QUANTUM EFFICIENCY FOR A BACK ILLUMINATED L3CCD

In the curve shown below are plotted the values of quantum efficiency we used in this memo.

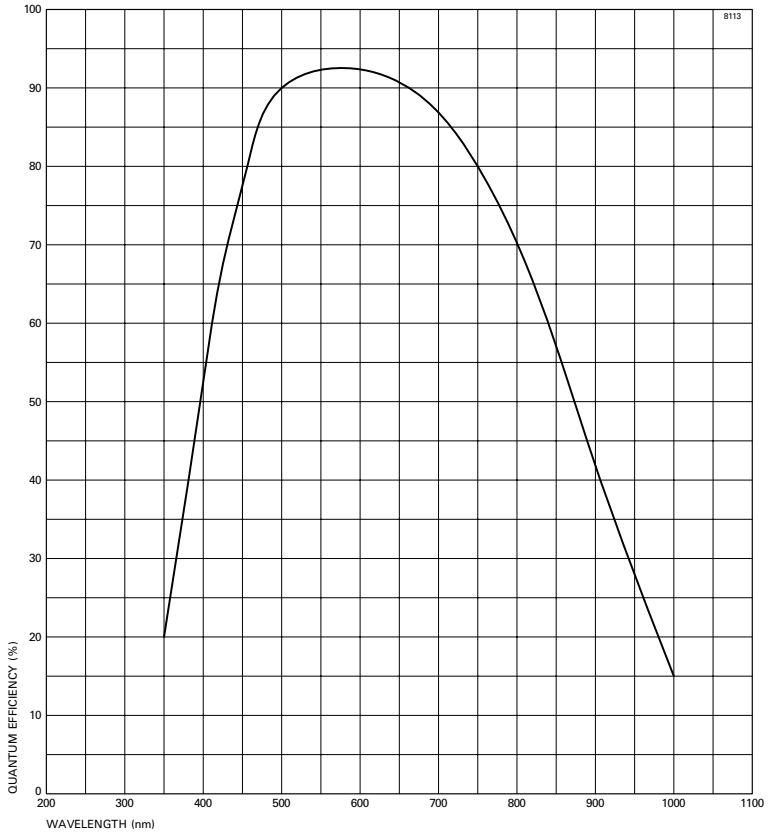

Figure 9. Plot of an L3CCD back illuminated quantum efficiency as a function of wavelength.

APPENDIX D. CENTROID ERROR

Roddier [1999] presents a slightly different estimator for the centroid tip-tilt error. He shows that from photon statistics, the rms error in measuring the centroid of an image due to Poisson and detector readout noise is proportional to 1/SNR (Roddier [1999, Eq. 12.41, p294]):

$$\sigma_c = \frac{c\gamma}{SNR}\frac{\lambda_t}{D} \tag{20}$$

where

$$c = \left[4\int_0^1 H(u,0)du\right]^{-1} \tag{21}$$

and λ_t is the mean sensing wavelength. H(u, v) is the optical transfer function of the imaging system. For a point source that is imaged through Kolmogorov turbulence with a circular aperture of diameter D,

$$H(u,0) = \frac{2}{\pi}exp\left[-3.44\left(\frac{D}{r_0}\right)^{5/3}u^{5/3}(1-u^{1/3})\right]\left[cos^{-1}(u) - u(1-u^2)^{1/2}\right]. \tag{22}$$

The factor SNR is the same as before.
This estimator requires less photons for the centroid error to be within the $0.0392(\lambda_i/D)$ threshold. We decided to use Olivier and Gavel's estimator in order to derive an upper limit for the required photon counts.

References

A. J. Horton, D. F. Buscher, and C. A. Haniff. Diffraction losses in ground-based optical interferometers. MNRAS, 327:217–226, October 2001.

C. W. McAlary, R. A. McLaren, R. J. McGonegal, and J. Maza. A near-infrared and optical study of X-ray selected Seyfert Galaxies. I - Observations. ApJS, 52:341–362, August 1983.

S. S. Olivier and D. T. Gavel. Tip-tilt compensation for astronomical imaging. *Optical Society of America Journal*, 11:368–378, January 1994.

A. Papoulis. *Probability, random variables and stochastic processes*. New York: McGraw-Hill, |c1965, 1965.

F. Roddier. *Adaptive optics in astronomy*. Adaptive optics in astronomy / edited by Francois Roddier. Cambridge ; New York, NY : Cambridge University Press, 1999, ISBN 052155375X, 1999.

D. G. Sandler, S. Stahl, J. R. P. Angel, M. Lloyd-Hart, and D. McCarthy. Adaptive optics for diffraction-limited infrared imaging with 8-m telescopes. *Optical Society of America Journal*, 11:925–945, February 1994.

W. J. Tango and R. Q. Twiss. Michelson stellar interferometry. In *Progress in optics. Volume 17. (A81-13109 03-74) Amsterdam, North-Holland Publishing Co., 1980, p. 239-277. Research supported by the Australian Research Grants Committee.*, pages 239–277, 1980.

G. A. Tyler. Bandwidth considerations for tracking through turbulence. *Optical Society of America Journal*, 11:358–367, January 1994.